Pavel Burda; Jaroslav Novotný; Jakub Šístek; Alexandr Damašek
Finite element modelling of some incompressible fluid flow problems

In: Jan Chleboun and Petr Přikryl and Karel Segeth and Tomáš Vejchodský (eds.): Programs and Algorithms of Numerical Mathematics, Proceedings of Seminar. Dolní Maxov, June 1-6, 2008. Institute of Mathematics AS CR, Prague, 2008. pp. 37–52.

Persistent URL: http://dml.cz/dmlcz/702854

FINITE ELEMENT MODELLING OF SOME INCOMPRESSIBLE FLUID FLOW PROBLEMS*

Pavel Burda, Jaroslav Novotný, Jakub Šístek, Alexandr Damašek

Abstract

We deal with modelling of flows in channels or tubes with abrupt changes of the diameter. The goal of this work is to construct the FEM solution in the vicinity of these corners as precise as desired. We present two ways. The first approach makes use of a posteriori error estimates and the adaptive strategy. The second approach is based on the asymptotic behaviour of the exact solution in the vicinity of the corner and on the a priori error estimate of the FEM solution. Then we obtain the solution with desired precision also in the vicinity of the corner, though there is a singularity. Numerical results are demonstrated on a 2D example.

1. Introduction

One of the challenging problems in fluid dynamics is reliable modelling of flows in channels or tubes with abrupt changes of the diameter, which appear often in engineering practice.

We present two ways for getting desired precision of the FEM solution in the vicinity of corners. Both make use of qualitative properties of the mathematical model of flow that is on the Navier-Stokes equations (NSE) for incompressible fluids.

The first approach makes use of a posteriori error estimates of the FEM solution which is carefully derived to trace the quality of the solution. Especially the constant in the a posteriori error estimate is investigated with care. Then we use the adaptive strategy to improve the mesh and thus to improve the FEM solution.

The second approach stands on two legs. One is the asymptotic behaviour of the exact solution of the NSE in the vicinity of the corner. This is obtained using some symmetry of the principal part of the Stokes equation and application of the Fourier transform. Second leg is the a priori error estimate of the FEM solution, where we estimate the seminorm of the exact solution by means of the above obtained asymptotics. On the mesh we then obtain the solution with desired precision also in the vicinity of the corner, though there is a singularity.

2. Navier-Stokes equations for incompressible viscous fluids

Let Ω be an open bounded domain in $\mathbb{R}^2$ filled with a fluid and let Γ be its Lipschitz continuous boundary. The generic point of $\mathbb{R}^2$ is denoted by $\mathbf{x} = (x_1, x_2)^T$ considered in meters and t denotes time variable considered in seconds.

*This work was supported by grant No. 106/08/0403 of the Czech Science Foundation and by the State Research Project No. MSM 684 0770010.

2.1. Unsteady two-dimensional flow

We deal with isothermal flow of Newtonian viscous fluids with constant density. Such flow is modelled by the Navier-Stokes system (nonconservative form):

$$\rho\left(\frac{\partial \mathbf{u}}{\partial t}+(\mathbf{u}\cdot\nabla)\mathbf{u}\right)-\mu\Delta\mathbf{u}+\nabla p_r = \rho\,\mathbf{f} \quad \text{in } \Omega\times[0,T], \tag{1}$$

$$\nabla\cdot\mathbf{u} = 0 \quad \text{in } \Omega\times[0,T], \tag{2}$$

where

- $\mathbf{u}=(u_1,u_2)^T$ denotes the vector of flow velocity [m/s], it is a function of $\mathbf{x}$ and t,
- p_r denotes the pressure [Pa], which is a function of $\mathbf{x}$ and t,
- ρ denotes the density of the fluid [kg/m^3],
- μ denotes the dynamic viscosity of the fluid [Pa·s], supposed to be constant,
- $\mathbf{f}=\mathbf{f}(\mathbf{x},t)$ is the density of volume forces per mass unit [N/m^3].

Dividing both sides of the momentum equation (1) by ρ and leaving the continuity equation (2) unchanged we obtain

$$\frac{\partial \mathbf{u}}{\partial t}+(\mathbf{u}\cdot\nabla)\mathbf{u}-\nu\Delta\mathbf{u}+\nabla p = \mathbf{f} \quad \text{in } \Omega\times[0,T], \tag{3}$$

$$\nabla\cdot\mathbf{u} = 0 \quad \text{in } \Omega\times[0,T], \tag{4}$$

where

- $p=p_r/\rho$ denotes the pressure divided by the density [Pa$\cdot$ m^3 /kg],
- $\nu=\mu/\rho$ denotes the kinematic viscosity of the fluid [m^2/s].

The system is supplied with the initial condition

$$\mathbf{u}=\mathbf{u}_0 \ \text{ in } \Omega,\ t=0, \tag{5}$$

where $\nabla\cdot\mathbf{u}_0=0$ and with the boundary conditions

$$\mathbf{u} = \mathbf{g} \ \text{ on } \Gamma_g\times[0,T], \tag{6}$$

$$-\nu(\nabla\mathbf{u})\mathbf{n}+p\mathbf{n} = \mathbf{0} \ \text{ on } \Gamma_h\times[0,T], \tag{7}$$

where

- Γ_g and Γ_h are two subsets of Γ satisfying $\overline{\Gamma}=\overline{\Gamma}_g\cup\overline{\Gamma}_h,\ \mu_{\mathbb{R}^1}(\Gamma_g\cap\Gamma_h)=0$,
- $\mathbf{n}$ denotes the unit outer normal vector to the boundary Γ.

Introduced $\mathbf{g}$ is a given function of $\mathbf{x}$ and t satisfying in the case of $\Gamma=\Gamma_g$ for all $t\in[0,T]$

$$\int_\Gamma \mathbf{g}\cdot\mathbf{n}\,\mathrm{d}\Gamma=0.$$

2.2. Steady 2D Navier-Stokes problem

In the case of steady two-dimensional flow, the Navier-Stokes equations are reduced to

$$(\mathbf{u}\cdot\nabla)\mathbf{u} - \nu\Delta\mathbf{u} + \nabla p = \mathbf{f} \quad \text{in } \Omega, \tag{8}$$

$$\nabla\cdot\mathbf{u} = 0 \quad \text{in } \Omega \tag{9}$$

and boundary conditions to

$$\mathbf{u} = \mathbf{g} \quad \text{on } \Gamma_g, \tag{10}$$

$$-\nu(\nabla\mathbf{u})\mathbf{n} + p\mathbf{n} = \mathbf{0} \quad \text{on } \Gamma_h. \tag{11}$$

2.3. Steady 2D Stokes problem

In the case of the Stokes flow the first (nonlinear) term in (8) is omitted:

$$-\nu\Delta\mathbf{u} + \nabla p = \mathbf{f} \quad \text{in } \Omega\ , \tag{12}$$

$$\nabla\cdot\mathbf{u} = 0 \quad \text{in } \Omega \tag{13}$$

and boundary conditions are the same as in (10), (11).

2.4. Variational formulation of Navier-Stokes equations

Let $L_2(\Omega)$ be the space of square integrable functions on Ω and let $L_2(\Omega)/\mathbb{R}$ be the space of functions in $L_2(\Omega)$ ignoring an additive constant. Let $H^1(\Omega)$ and $H_0^1(\Omega)$ be the Sobolev spaces defined as

$$H^1(\Omega) \equiv \left\{ v \mid v \in L^2(\Omega), \frac{\partial v}{\partial x_i} \in L^2(\Omega), i = 1,2 \right\},$$

$$H_0^1(\Omega) \equiv \left\{ v \mid v \in H^1(\Omega), \mathbf{Tr}\ v = 0 \right\},$$

where $\mathbf{Tr}$ is the trace operator $\mathbf{Tr}:\ H^1(\Omega) \longrightarrow L_2(\Gamma)$ and derivatives are considered in the weak sense.

The inner product and norm in the space $L_2(\Omega)$ are defined as

$$(u,v)_{L_2(\Omega)} \equiv \int_\Omega uv\ \mathrm{d}\Omega\ , \qquad \|v\|^2_{L_2(\Omega)} \equiv \int_\Omega v^2 \mathrm{d}\Omega$$

and the norm of function v in the Sobolev space $H^1(\Omega)$ is considered as

$$\|v\|^2_{H^1(\Omega)} \equiv \int_\Omega \left(v^2 + \sum_{k=1}^{2} \left(\frac{\partial v}{\partial x_k} \right)^2 \right) \mathrm{d}\Omega\ .$$

Sometimes, the notation $\|\cdot\|_{L_2(\Omega)}$ is shortened to $\|\cdot\|_0$ and $\|\cdot\|_{H^1(\Omega)}$ to $\|\cdot\|_1$. Similarly, the notation $(u,v)_{L_2(\Omega)}$ is shortened to $(u,v)_0$.

Let us define vector function spaces V_g and V by

$$\begin{aligned} V_g &\equiv \left\{ \mathbf{v} = (v_1, v_2)^T \mid \mathbf{v} \in [H^1(\Omega)]^2; \mathbf{Tr}\ v_i = g_i, i = 1, 2 \right\} , \\ V &\equiv \left\{ \mathbf{v} = (v_1, v_2)^T \mid \mathbf{v} \in [H_0^1(\Omega)]^2 \right\} . \end{aligned}$$

Let us note, that the norm of vector function $\mathbf{v}$ in the spaces V_g and V is then

$$\|\mathbf{v}\|^2_{[H^1(\Omega)]^2} \equiv \sum_{i=1}^{2} \int_\Omega \left(v_i^2 + \sum_{k=1}^{2} \left(\frac{\partial v_i}{\partial x_k} \right)^2 \right) \mathrm{d}\Omega$$

and the norm of vector function $\mathbf{v}$ in the space $[L_2(\Omega)]^2$ is

$$\|\mathbf{v}\|^2_{[L_2(\Omega)]^2} \equiv \sum_{i=1}^{2} \int_\Omega v_i^2 \mathrm{d}\Omega \ .$$

The *weak unsteady Navier-Stokes problem* means seeking of $\mathbf{u}(t) \in V_g$, $\mathbf{u}(t) = (u_1(t), u_2(t))^T$, and $p(t) \in L_2(\Omega)/\mathbb{R}$ satisfying for any $t \in [0, T]$ and $\forall\ \mathbf{v} \in V$ and $\forall\ \psi \in L^2(\Omega)$:

$$\int_\Omega \frac{\partial \mathbf{u}}{\partial t} \cdot \mathbf{v} \mathrm{d}\Omega + \int_\Omega (\mathbf{u} \cdot \nabla)\mathbf{u} \cdot \mathbf{v} \mathrm{d}\Omega + \nu \int_\Omega \nabla \mathbf{u} : \nabla \mathbf{v} \mathrm{d}\Omega - \int_\Omega p \nabla \cdot \mathbf{v} \mathrm{d}\Omega = \int_\Omega \mathbf{f} \cdot \mathbf{v} \mathrm{d}\Omega \ , \tag{14}$$

$$\int_\Omega \psi \nabla \cdot \mathbf{u} \mathrm{d}\Omega = 0 \ , \tag{15}$$

$$\mathbf{u} - \mathbf{u}_g \in V. \tag{16}$$

The operation $\nabla \mathbf{u} : \nabla \mathbf{v}$ is defined as

$$\nabla \mathbf{u} : \nabla \mathbf{v} \equiv \frac{\partial u_x}{\partial x}\frac{\partial v_x}{\partial x} + \frac{\partial u_x}{\partial y}\frac{\partial v_x}{\partial y} + \frac{\partial u_y}{\partial x}\frac{\partial v_y}{\partial x} + \frac{\partial u_y}{\partial y}\frac{\partial v_y}{\partial y} \ .$$

Similarly, the *weak steady Navier-Stokes problem* reads:
Seek $\mathbf{u} = (u_1, u_2)^T \in V_g$ and $p \in L_2(\Omega)/\mathbb{R}$ satisfying $\forall\ \mathbf{v} \in V$ and $\forall\ \psi \in L^2(\Omega)$:

$$\int_\Omega (\mathbf{u} \cdot \nabla)\mathbf{u} \cdot \mathbf{v} \mathrm{d}\Omega + \nu \int_\Omega \nabla \mathbf{u} : \nabla \mathbf{v} \mathrm{d}\Omega - \int_\Omega p \nabla \cdot \mathbf{v} \mathrm{d}\Omega = \int_\Omega \mathbf{f} \cdot \mathbf{v} \mathrm{d}\Omega \ , \tag{17}$$

$$\int_\Omega \psi \nabla \cdot \mathbf{u} \mathrm{d}\Omega = 0 \ , \tag{18}$$

$$\mathbf{u} - \mathbf{u}_g \in V. \tag{19}$$

In case of the *weak steady Stokes problem* instead of (17) we require

$$\nu \int_\Omega \nabla \mathbf{u} : \nabla \mathbf{v} \mathrm{d}\Omega - \int_\Omega p \nabla \cdot \mathbf{v} \mathrm{d}\Omega = \int_\Omega \mathbf{f} \cdot \mathbf{v} \mathrm{d}\Omega \ . \tag{20}$$

3. Finite element method for Navier-Stokes equations

Let us divide the domain Ω (supposed to be polygonal from now) into N elements T_K, $K = 1, 2, \ldots, N$, of a triangulation $\mathcal{T}$ such that

$$\begin{aligned} \bigcup_{K=1}^{N} \overline{T}_K &= \overline{\Omega}\ , \\ \mu_{\mathbb{R}^2}\left(T_K \cap T_L\right) &= 0, \quad K \neq L\ . \end{aligned}$$

Let h_K mean the diameter of the element T_K.

3.1. Function spaces for velocity and pressure approximation

To solve the Navier-Stokes equations, different polynomial approximation for velocities and for pressure are usually chosen. Equal order approximation is easy to implement, but pressure exhibits instability. Approximation with different order is more suitable for practical computing, cf. [3]. I. Babuška and F. Brezzi introduced a condition (also called *inf-sup* condition) limitting the choice of combinations of approximation

$$\exists C_B > 0, const.\ \forall q_h \in Q_h\ \exists \mathbf{v}_h \in V_{gh}\ (q_h, \nabla \cdot \mathbf{v}_h)_0 \geq C_B \|q_h\|_0 \|\mathbf{v}_h\|_1\ , \tag{21}$$

where Q_h and V_{gh} are the function spaces for approximation of pressure and velocity. Condition (21) is important for stability. It is satisfied, e.g., for Taylor-Hood elements we use.

3.2. Taylor-Hood finite elements

In this paper we apply Taylor-Hood finite elements on triangles and quadrilaterals. Values of velocity are approximated at corner nodes and midsides and values of pressure at corner nodes (Figure 1). It corresponds to the following function spaces on element T_K:

- *triangle*
  $v_i \in P_2(T_K)$, $i = 1, 2$, i.e. polynomials of the second order,
  $p \in P_1(T_K)$, i.e. linear polynomials
- *quadrilateral*
  $v_i \in Q_2(T_K)$, $i = 1, 2$, i.e. polynomials of the second order for each coordinate,
  $p \in Q_1(T_K)$, i.e. bilinear polynomials.

Let us employ the notation

$$R_m(\overline{T_K}) = \begin{cases} P_m(\overline{T_K}), & \text{if } T_K \text{ is a triangle} \\ Q_m(\overline{T_K}), & \text{if } T_K \text{ is a quadrilateral} \end{cases} \tag{22}$$

and let $\mathcal{C}(\overline{\Omega})$ denote the space of continuous functions on $\overline{\Omega}$.

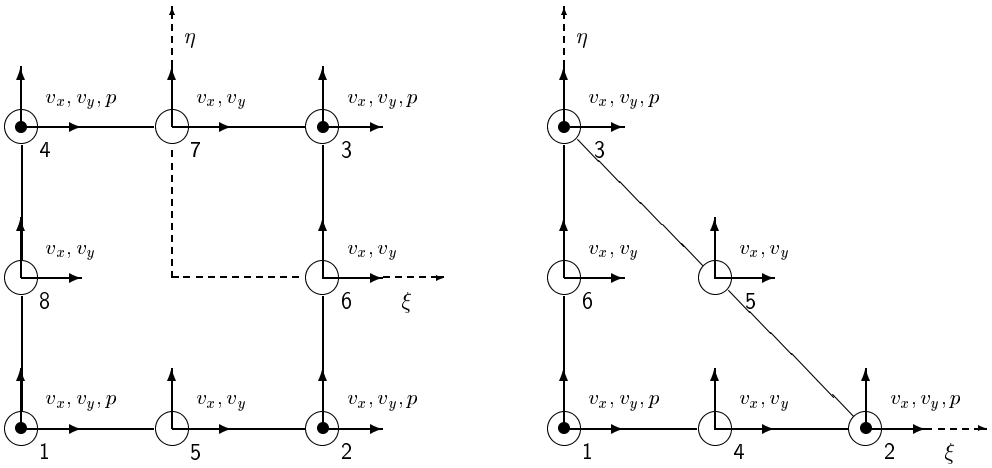

Fig. 1: *Taylor-Hood reference elements.*

Application of Taylor-Hood finite elements leads to the final approximation on the domain Ω satisfying $\mathbf{u}_h \in V_{gh}$ and $p_h \in Q_h$ where

$$V_{gh} = \Big\{ \mathbf{v}_h = (v_{h_1}, v_{h_2})^T \in [\mathcal{C}(\overline{\Omega})]^2;\ v_{h_i}\,|_{T_K} \in R_2(\overline{T_K}),\ K = 1, \ldots, N,\ i = 1, 2, \quad (23)$$
$$\mathbf{v}_h = \mathbf{g} \text{ at nodes on } \Gamma \Big\} ,$$
$$Q_h = \Big\{ \psi_h \in \mathcal{C}(\overline{\Omega});\ \psi_h\,|_{T_K} \in R_1(\overline{T_K}),\ K = 1, \ldots, N \Big\} . \quad (24)$$

We also need the space

$$V_h = \Big\{ \mathbf{v}_h = (v_{h_1}, v_{h_2})^T \in [\mathcal{C}(\overline{\Omega})]^2;\ v_{h_i}\,|_{T_K} \in R_2(\overline{T_K}),\ K = 1, \ldots, N,\ i = 1, 2, \quad (25)$$
$$\mathbf{v}_h = \mathbf{0} \text{ at nodes on } \Gamma \Big\} .$$

Since these spaces satisfy $V_{gh} \subset V_g$, $V_h \subset V$, and $Q_h \subset L_2(\Omega)/\mathbb{R}$ for prescribed arbitrary value of pressure (e.g. $p_h = 0$) in one node, we can introduce *approximate steady Navier-Stokes problem*:
Seek $\mathbf{u}_h \in V_{gh}$ and $p_h \in Q_h$ satisfying

$$\int_\Omega (\mathbf{u}_h \cdot \nabla)\mathbf{u}_h \cdot \mathbf{v}_h \mathrm{d}\Omega + \nu \int_\Omega \nabla \mathbf{u}_h : \nabla \mathbf{v}_h \mathrm{d}\Omega - \int_\Omega p_h \nabla \cdot \mathbf{v}_h \mathrm{d}\Omega = \int_\Omega \mathbf{f} \cdot \mathbf{v}_h \mathrm{d}\Omega,\ \forall \mathbf{v}_h \in V_h, \quad (26)$$

$$\int_\Omega \psi_h \nabla \cdot \mathbf{u}_h \mathrm{d}\Omega = 0,\ \forall \psi_h \in Q_h\ , \quad (27)$$

$$\mathbf{u}_h - \mathbf{u}_{gh} \in V_h\ , \quad (28)$$

where $\mathbf{u}_{gh} \in V_{gh}$ is the projection of $\mathbf{u}_g$ onto the space V_{gh}.

Similarly we define *approximate steady Stokes problem*, just omitting the first term in (26).

Using the shape-regular triangulation and refining the mesh such that $h_{\max} \to 0$, where

$$h_{\max} = \max_K h_K,$$

the solution of the approximated problem converges to the solution of the continuous problem (for more detail see e.g. [3]).

4. Asymptotic behaviour of the solution near corners

We are concerned with flow in tubes and channels with abrupt changes of diameter. The results are based on the paper [4], where we investigated *the pipe flow* (axisymmetric). The asymptotic behaviour of *plane flow* with corner singularities was studied e.g. by Kondratiev [17]. The asymptotics of the biharmonic equation for the stream function ψ are basic. Let us e.g. take the case of the nonconvex domain with the internal angle $\omega = \frac{3}{2}\pi$, cf. Figure 2. Then, in polar coordinates we get the expansion

$$\psi(\rho, \vartheta) = \rho^{1.54448374}\ \phi(\vartheta)\ +\ \ldots\ (\textit{lower order terms}), \tag{29}$$

where ρ is the distance from the corner, see [4]. This result is the same as that obtained in desk geometry by Kondratiev [17], where

$$\psi^{desk}(\rho, \vartheta) = \rho^{1.5445}\ \phi^d(\vartheta)\ +\ \ldots\ (l.o.t.). \tag{30}$$

So we get the expansion for the velocities:

$$u_l(\rho, \vartheta) = \rho^{0.54448374}\varphi_l(\vartheta) + \ldots (l.o.t.)\ ,\ l = 1, 2, \tag{31}$$

where the functions φ_l do not depend on ρ, the distance from the corner. This expansion exhibits the infinite gradient of velocity near the corner.

In Section 6 our aim is to make use of the information on the local behaviour of the solution near the corner point, in order to design local meshing subordinate to the asymptotics.

5. A posteriori error estimates for the Navier-Stokes equation

At present various a posteriori error estimates for the Stokes and Navier-Stokes problems are available. We mention e.g. Babuška, Rheinboldt [2], Ainsworth, Oden [1], Verfürth [19]. Other references can be found in [5].

5.1. A posteriori estimates for 2D steady Navier-Stokes equations

Let us consider the steady Navier-Stokes problem (8), (9), with boundary conditions (10), (11).

For the discretization by finite elements we use again Taylor-Hood elements P2/P1.

Suppose that exact solution of the problem is denoted by (u_1, u_2, p) and the approximate finite element solution by (u_1^h, u_2^h, p_h). The exact solution differs from the approximate solution in the error

$$(e_{u_1}, e_{u_2}, e_p) \equiv (u_1 - u_1^h, u_2 - u_2^h, p - p_h). \tag{32}$$

For the solution (u_1, u_2, p) we denote

$$\begin{aligned} &\mathcal{U}^2(u_1, u_2, p, \Omega) \equiv \|(u_1, u_2, p)\|_V^2 \equiv \|(u_1, u_2)\|_{1,\Omega}^2 + \|p\|_{0,\Omega}^2 \qquad (33)\\ &\equiv \int_\Omega \left(u_1^2 + u_2^2 + \left(\frac{\partial u_1}{\partial x}\right)^2 + \left(\frac{\partial u_1}{\partial y}\right)^2 + \left(\frac{\partial u_2}{\partial x}\right)^2 + \left(\frac{\partial u_2}{\partial y}\right)^2 \right) \mathrm{d}\Omega + \int_\Omega p^2 \mathrm{d}\Omega. \end{aligned}$$

The estimate proved in [5], [6], [7] for the Stokes problem can be generalized to the Navier-Stokes equations:

$$\|(e_{u_1}, e_{u_2})\|_{1,\Omega}^2 + \|e_p\|_{0,\Omega}^2 \le \mathcal{E}^2(u_1^h, u_2^h, p^h), \tag{34}$$

where (cf. [19])

$$\mathcal{E}^2(u_1^h, u_2^h, p^h, \Omega) \equiv C \left[\sum_{K \in \mathcal{T}^h} h_K^2 \int_{T_K} \left(r_1^2 + r_2^2\right) + \sum_{K \in \mathcal{T}^h} \int_{T_K} r_3^2 \mathrm{d}\Omega \right], \tag{35}$$

where h_K denotes the diameter of the element T_K and $r_i,\ i = 1, 2, 3$, are the residuals

$$r_1 = f_x - \left(u_1^h \frac{\partial u_1^h}{\partial x} + u_2 \frac{\partial u_1^h}{\partial y} \right) + \nu \left(\frac{\partial^2 u_1^h}{\partial x^2} + \frac{\partial^2 u_1^h}{\partial y^2} \right) - \frac{\partial p^h}{\partial x}, \tag{36}$$

$$r_2 = f_y - \left(u_1^h \frac{\partial u_2^h}{\partial x} + u_2^h \frac{\partial u_2^h}{\partial y} \right) + \nu \left(\frac{\partial^2 u_2^h}{\partial x^2} + \frac{\partial^2 u_2^h}{\partial y^2} \right) - \frac{\partial p^h}{\partial y}, \tag{37}$$

$$r_3 = \frac{\partial u_1^h}{\partial x} + \frac{\partial u_2^h}{\partial y}. \tag{38}$$

Let us note that due to our practical experience we use only the element residuals.

Denote also

$$\mathcal{E}^2(u_1^h, u_2^h, p^h, T_K) \equiv C \left[h_K^2 \int_{T_K} \left(r_1^2 + r_2^2\right) + \int_{T_K} r_3^2 \mathrm{d}\Omega \right]. \tag{39}$$

It is important, that C does not depend on the mesh size and so can be determined experimentally for general situation.

By computing of the estimates (11) we obtain absolute numbers, that will depend on given quantities in different problems. We are mainly interested in the error related to the computed solution, i.e. relative error. This is given by the ratio of the absolute norm of the solution error related to the unit area of the element T_K, $\frac{1}{|T_K|}\ \mathcal{E}^2(u_1^h, u_2^h, p^h, T_K)$, and the solution norm on the whole domain Ω, related to unit area $\frac{1}{|\Omega|}\ \|(u_1^h, u_2^h, p^h)\|^2_{V,\Omega}$, i.e.

$$\mathcal{R}^2(u_1^h, u_2^h, p^h, T_K) = \frac{|\Omega|\ \mathcal{E}^2(u_1^h, u_2^h, p^h, T_K)}{|T_K|\ \|(u_1^h, u_2^h, p^h)\|^2_{V,\Omega}}. \tag{40}$$

5.2. Determination of the constant C

In papers [7], [8] we investigated the problem of the constant C in the a posteriori estimates. Comparing analytical and finite element solution of some model problems we found the appropriate value of the constant. For details we refer to [7] and [8].

5.3. Numerical results and application of estimates to the construction of adaptive meshes

Consider two-dimensional flow of viscous, incompressible fluid described by Navier-Stokes equations in domain with corner singularity, cf. Figure 2.

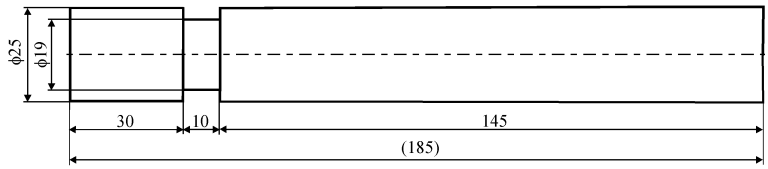

Fig. 2: *Geometry of the channel.*

Due to the symmetry, we solve the problem only on half of the channel, cf. Figure 3. On the inflow we consider parabolic velocity profile, on the outflow 'do nothing' boundary condition. On the upper wall no-slip condition and on the lower wall condition of symmetry (i.e. only y-component of velocity equals zero). We consider the following parameters: $\nu = 0.0001$ m^2/s, $u_{in} = 1$ m/s. The initial mesh is in Figure 3.

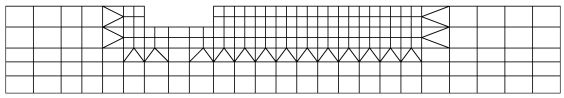

Fig. 3: *Initial finite element mesh.*

Elements, where the relative error by (40) exceeds 3 %, are refined and new solution together with new error estimates is computed. The third refinement is seen in Figure 4.

The relative errors in the vicinity of the left corner are shown in Figure 5.

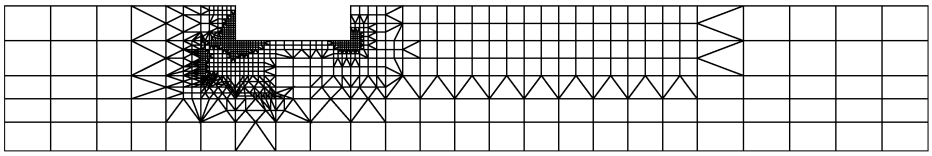

Fig. 4: *Finite element mesh after third refinement.*

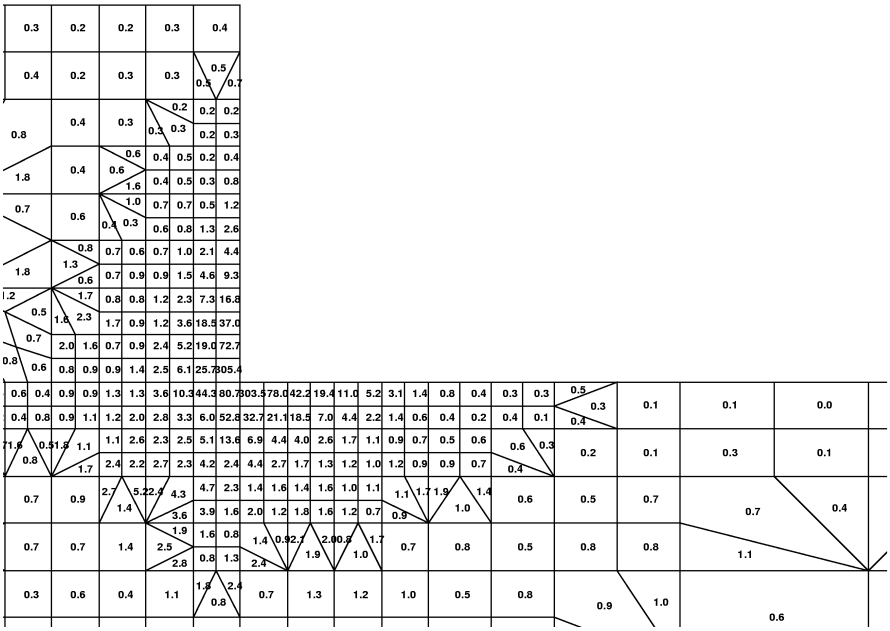

Fig. 5: *Relative errors on elements of the third refinement.*

Numerical results of velocity components and pressure are in Figures 6 and 7. The corner singularities caused by nonconvex corners are approximated with the accuracy indicated in Figure 5.

6. Application of a priori estimates for Navier-Stokes equations

The goal of this section is to summarize authors' experience with the application of a priori error estimates of the finite element method in computational fluid dynamics. This approach is applied to generate the computational mesh in the purpose of uniform distribution of error on elements and is used in precise solution on domains with corner-like singularities. Incompressible viscous flow modelled by the steady Navier-Stokes equations (17)–(19) is considered.

One possible way to improve accuracy of solution by the FEM is to refine the mesh near places, where singularity can appear, by means of adaptive refinement based on a posteriori error estimates or error estimators, as presented in Section 5. This method could be quite time demanding, since it needs several runs of solu-

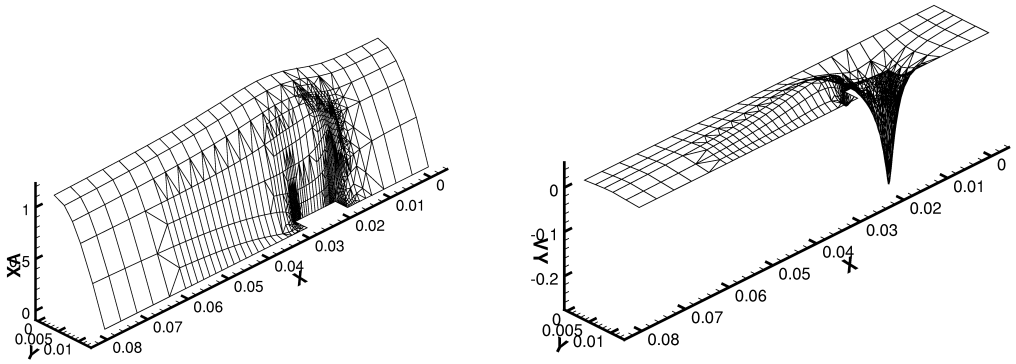

Fig. 6: *After third refinement: velocity u_x (left) and velocity u_y (right).*

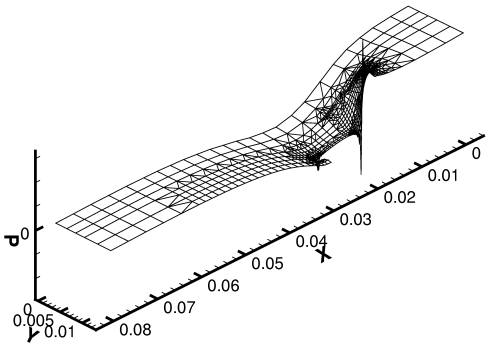

Fig. 7: *Pressure p after third refinement.*

tion. Completely different method is applied in this section. Computational mesh is prepared before the first run of the solution.

Numerical results are presented for flows in a channel with sharp obstacle and in a channel with sharp extension. Let us note that some other results were published in [9].

6.1. Algorithm for generation of computational mesh

In the derivation of the algorithm, two main 'tools' are used. The first is a priori estimate of the finite element error for the Navier-Stokes equations (17)–(19) (cf. [13]),

$$\|\nabla(\mathbf{u}-\mathbf{u_h})\|_{L_2(\Omega)} \le C\Big[\Big(\sum_K h_K^{2k} \mid \mathbf{u} \mid^2_{H^{k+1}(T_K)}\Big)^{1/2} + \Big(\sum_K h_K^{2k} \mid p \mid^2_{H^k(T_K)}\Big)^{1/2}\Big] , \quad (41)$$

$$\|p-p_h\|_{L_2(\Omega)} \le C\Big[\Big(\sum_K h_K^{2k} \mid \mathbf{u} \mid^2_{H^{k+1}(T_K)}\Big)^{1/2} + \Big(\sum_K h_K^{2k} \mid p \mid^2_{H^k(T_K)}\Big)^{1/2}\Big] , \quad (42)$$

where h_K is the diameter of triangle T_K of a triangulation $\mathcal{T}$ and $k = 2$ for Taylor-Hood elements, which are applied in presented numerical experiments.

The second tool is the asymptotic behaviour of the solution near the singularity. In Section 4.2 (see also [4]), it was proved for the Stokes flow in axisymmetric tubes, that for internal angle $\alpha = \frac{3}{2}\pi$, the leading term of expansion of the solution for each velocity component is

$$u_i(\rho, \vartheta) = \rho^{0.5445}\varphi_i(\vartheta) + \dots \ (l.o.t.),\ i = 1, 2\ , \tag{43}$$

where ρ is the distance from the corner, ϑ is the angle and φ_i is a smooth function. The same expansion is known to apply to the plane flow (cf. [16]) and similar results were also proved for the Navier-Stokes equations. Differentiating by ρ, we observe $\frac{\partial u_i(\rho,\vartheta)}{\partial \rho} \ \to \ \infty$ for $\rho \ \to \ 0$.

Taking into account the expansion (43), we can estimate

$$|\ \mathbf{u}\ |^2_{H^{k+1}(T_K)} \approx C \int\limits_{r_K - h_K}^{r_K} \rho^{2(\gamma-k-1)}\ \rho\ d\rho = C\ \left[-r_K^{2(\gamma-k)} + (r_K - h_K)^{2(\gamma-k)}\right]\ , \tag{44}$$

where r_K is the distance of element T_K from the corner, cf. Figure 8.

Putting estimate (44) into the a priori error estimate (41) or (42), we derive that we should guarantee

$$h_K^{2k}\left[-r_K^{2(\gamma-k)} + (r_K - h_K)^{2(\gamma-k)}\right] \approx h_{ref}^{2k}\ , \tag{45}$$

in order to get the error estimate of order $O(h_{ref}^k)$ uniformly distributed on elements. From this expression, we compute element diameters using the Newton method in accordance to chosen h_{ref}. Similar idea was presented by C. Johnson for an elliptic problem in [15].

6.2. Geometry and design of the mesh

The algorithm was applied to the channel with sudden intake of diameter (see Figure 2). Due to symmetry, again the problem was solved only on the upper half of the channel.

The diameters of elements were computed for values $h_{ref} = 0.1732$ mm, $k = 2$, $\gamma = 0.5444837$. We started in the distance $r_1 = 0.25$ mm from the corner. This corresponds to cca 3 % of relative error on elements. Fourteen diameters of elements were obtained. The detail of the mesh refinement is in Figure 8. More in [8].

The refined detail is connected to the rest of the coarse mesh. In Figure 9 final mesh after the refinement is shown.

6.3. Measuring of error

To review the efficiency of the algorithm, we use a posteriori error estimates as derived in Chapter 5, to evaluate the obtained error on elements. Suppose that the exact solution of the problem is denoted as (u_1, u_2, p) and the approximate solution

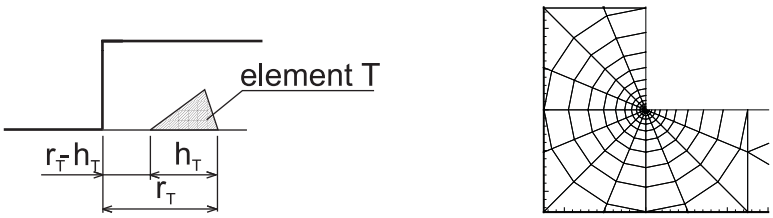

Fig. 8: *Description of element variables (left), details of refined mesh (right).*

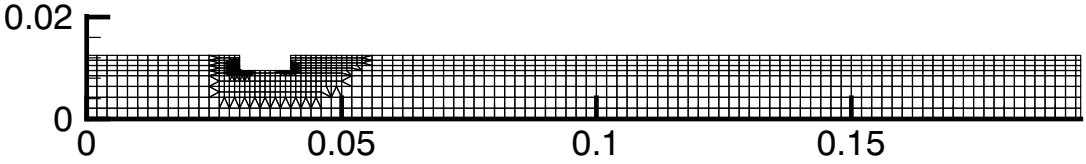

Fig. 9: *Final computational mesh for the channel.*

obtained by the FEM as (u_1^h, u_2^h, p^h). The exact solution differs from the approximate solution in the error $(e_{u_1}, e_{u_2}, e_p) = (u_1 - u_1^h, u_2 - u_2^h, p - p^h)$.

In adaptive mesh refinement in Sections 5.3–5.5 we used the error estimator (40). In this chapter, for the similarity with a priori error estimate, we use the modified absolute error defined as

$$\mathcal{A}_m^2(u_{1h}, u_{2h}, p_h, T_K, \Omega, n) = \frac{|\Omega| \mathcal{E}^2(u_{1h}, u_{2h}, p_h, T_K)}{|\overline{T_K}|\ \mathcal{U}^2(u_{1h}, u_{2h}, p_h, \Omega)}\ , \tag{46}$$

where $|\overline{T_K}|$ is the mean area of elements obtained as $|\overline{T_K}| = \frac{|\Omega|}{n}$, where n denotes the number of all elements in the domain and the symbols $\mathcal{E}^2(u_{1h}, u_{2h}, p_h, T_K)$, $\mathcal{U}^2(u_{1h}, u_{2h}, p_h, \Omega)$ are defined in (33), (39).

6.4. Numerical results

Channel with sudden intake of diameter (results for Re = 1000)

In Figures 10-11, plots of entities that characterize the flow in the channel are presented. In Figure 10, there are streamlines and a plot of the velocity component u_x. Plots of velocity component u_y and pressure are in Figure 11. Note, that the fluid flows from the right to the left on plots of u_x, u_y, and p for better view. Let us note that the relative error on the elements never exceeded 3 %. So the corner singularities caused by nonconvex corners are approximated here with very high accuracy.

7. Conclusion

Presented work is mainly focused on flow problems with singularities caused by corners in the solution domain and on the construction of the FEM solution in the vicinity of these corners as precisely as desired.

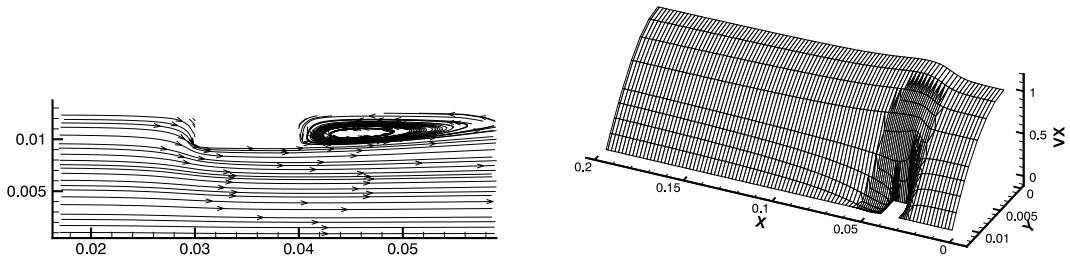

Fig. 10: *Detail of streamlines (left) and velocity component u_x (right).*

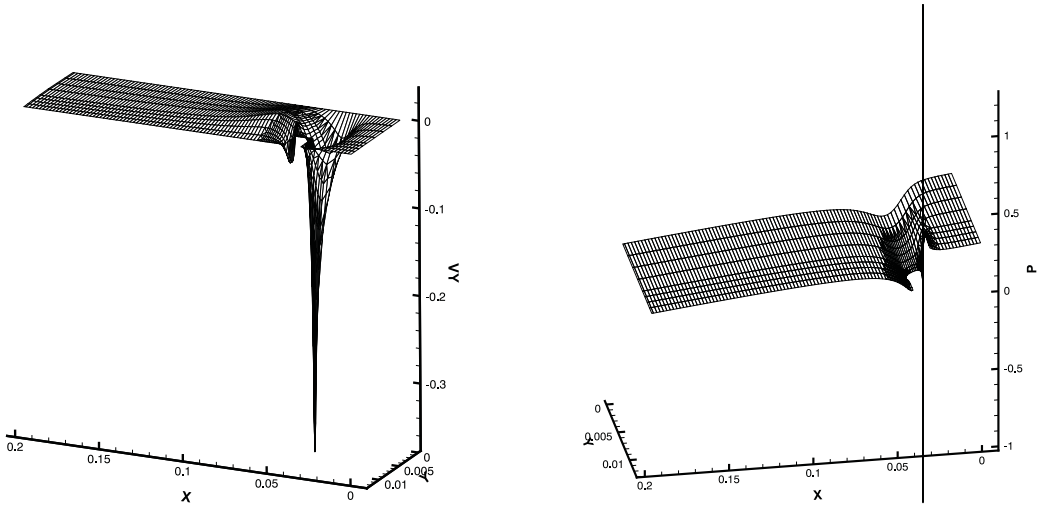

Fig. 11: *Velocity component u_y (left) and pressure (right).*

We presented two ways for getting desired precision of the FEM solution in the vicinity of corners. Both make use of qualitative properties of the mathematical model of flow. As a mathematical model we accept the Navier-Stokes equations (NSE) for incompressible fluids.

The first approach described in Section 5 makes use of a posteriori error estimates of the FEM solution which is carefully derived to trace the quality of the solution. Especially the constant in the a posteriori estimate is investigated with care. Then we use the adaptive strategy to improve the mesh and thus to improve the FEM solution. Numerical results demonstrate the robustness of this approach.

The second approach stands on two columns. In Section 4 we gave the asymptotic behaviour of the exact solution of the NSE in the vicinity of the corner. This is obtained using some symmetry of the principal part of the Stokes equation, then applying the Fourier transform and investigating the resolvent of the corresponding operator. Second column is the a priori error estimate of the FEM solution, where we estimate the seminorm of the exact solution by means of the above obtained asymptotics. In Section 6, according to these ideas, we derive an algorithm for designing the FEM mesh in advance (a priori). On the mesh we then obtain the

solution with desired precision, namely in the vicinity of the corner, though there is a singularity.

The applications in Section 6 confirm the achievement of the goal – to obtain solution tinged with errors on elements satisfactorily small and uniformly distributed. Using this approach, we can save a lot of computational time using mesh 'prepared' for expected solution.

Recently we dealt also with the stabilized version of FEM to enable the calculation of flows with higher Reynolds numbers [10], [11]. We also combined stabilization with presented achievements on a posteriori error estimates. Our achievements with precise solution of problems with singularities may serve as an important tool for verification, see [12].

References

[1] M. Ainsworth, J.T. Oden: *A posteriori error estimators for the Stokes and Oseen equations*. SIAM J. Numer. Anal., **34** (1997) 228–245.

[2] I. Babuška, W.C. Rheinboldt: *A posteriori error estimates for the finite element method*. Internat. J. Numer. Meth. Engrg., **12** (1978) 1597–1615.

[3] F. Brezzi, M. Fortin: *Mixed and hybrid finite element methods*, Springer, Berlin, 1991.

[4] P. Burda: *On the FEM for the Navier-Stokes equations in domains with corner singularities*. In: M. Křížek et al. (Eds), *Finite Element Methods, Supeconvergence, Post-Processing and A Posteriori Estimates*, Marcel Dekker, New York, 1998, pp. 41–52.

[5] P. Burda: *An a posteriori error estimate for the Stokes problem in a polygonal domain using Hood-Taylor elements.* In: P. Neittaanmäki et al. (Eds) *ENUMATH 99, Proc. of the 3-rd European Conference on Numerical Mathematics and Advanced Applications.* World Scientific, Singapore, 2000, pp. 448–455.

[6] P. Burda: *A posteriori error estimates for the Stokes flow in 2D and 3D domains*. In: P. Neittaanmäki, M. Křížek (eds), *Finite Element Methods, 3D.* (GAKUTO Internat. Series, Math. Sci. and Appl., Vol. 15), Gakkotosho, Tokyo, 2001, pp. 34–44.

[7] P. Burda, J. Novotný, B. Sousedík: *A posteriori error estimates applied to flow in a channel with corners*, Math. Comput. Simulation **61** (2003), 375–383.

[8] P. Burda, J. Novotný, B. Sousedík, J. Šístek: *Finite element mesh adjusted to singularities applied to axisymmetric and plane flow*. In: M. Feistauer et al. (Eds), *Numerical Mathematics and Advanced Applications, ENUMATH 2003*, Springer, Berlin, 2004, pp. 186–195.

[9] P. Burda, J. Novotný, J. Šístek: *Precise FEM solution of corner singularity using adjusted mesh applied to axisymmetric and plane flow*, ICFD Conf. on Num. Meth. for Fluid Dynamics, Univ. Oxford, March 2004, Internat. J. Numer. Methods Fluids, **47** (2005), 1285–1292.

[10] P. Burda, J. Novotný, J. Šístek: *On a modification of GLS stabilized FEM for solving incompressible viscous flows*, Fef05, Swansea, March 2005, Internat. J. Numer. Methods Fluids, **51** (2006), 1001–1016.

[11] P. Burda, J. Novotný, J. Šístek: *Numerical solution of flow problems by stabilized finite element method and verification of its accuracy using a posteriori error estimates*, Math. Comput. Simulation **76** (2007), 28–33.

[12] P. Burda, J. Novotný, J. Šístek: *Accuracy of semiGLS stabilization of FEM for solving Navier-Stokes equations and a posteriori error estimates*, Internat. J. Numer. Methods Fluids, **56** (2008), 1167–1173.

[13] V. Girault, P.G. Raviart: *Finite element method for Navier-Stokes equations*, Springer, Berlin, 1986.

[14] R. Glowinski: *Finite element methods for incompressible viscous flow*, Handbook of Numerical Analysis, Vol. IX, Elsevier, 2003.

[15] C. Johnson: *Numerical solution of partial differential equations by the finite element method*, Cambridge University Press, 1994.

[16] V.A. Kondratiev: *Asimptotika rešenija uravnienija Nav'je-Stoksa v okrestnosti uglovoj točki granicy*, Prikl. Mat. i Mech., **1** (1967), 119–123

[17] V.A. Kondratiev: *Krajevyje zadači dlja elliptičeskich uravněnij v oblasťach s koniěskimi i uglovymi točkami*, Trudy Moskov. Mat. obshch. 16 (1967), 209–292.

[18] J. Šístek: *Stabilization of finite element method for solving incompressible viscous flows*, Diploma thesis, ČVUT, Praha, 2004.

[19] R. Verfürth: *A Review of A Posteriori Error Estimation and Adaptive Mesh-Refinement Techniques*, Wiley and Teubner, Chichester, 1996.